Progress In Electromagnetics Research C, Vol. 154, 249–255, 2025

PIER C

(Received 3 March 2025, Accepted 15 April 2025, Scheduled 22 April 2025)

Measurement Matrix Optimization for Compressive Sensing-Based Method of Moments Based on Dynamic Extraction

Zhonggen Wang[1], Yang Liu[1,*], and Wenyan Nie[2]

[1]School of Electrical and Information Engineering, Anhui University of Science and Technology, Huainan 232001, China
[2]School of Mechanical and Electrical Engineering, Huainan Normal University, Huainan 232001, China

ABSTRACT: To address the challenges in constructing the measurement matrix within the compressive sensing-based method of moments (CS-MoM) framework, this paper presents a novel dynamic extraction method based on row norm significance for impedance matrix compression. The proposed method first sorts the impedance matrix rows in descending order according to their row norm importance, followed by a dynamic extraction process that adapts the extraction density based on row significance. This strategy ensures dense extraction of high-importance rows to maintain matrix representativeness, while sparse extraction of low-importance rows preserves global structural coverage. Finally, through the validation of numerical results from three different computational models, it is demonstrated that the proposed method improves computational accuracy while ensuring computational efficiency compared to the uniform extraction-based novel CS-MoM method.

1. INTRODUCTION

The method of moments (MoM) [1] is an effective numerical approach for analyzing electromagnetic scattering from targets; however, it incurs unacceptable computational costs when being applied to problems involving electrically large targets. Consequently, several acceleration algorithms have been proposed, including multilevel fast multipole method [2], high-level MoM [3], and characteristic basis function method [4–6]. Unlike these acceleration algorithms, compressive sensing (CS) [7], an emerging technique for reducing computational complexity, has been integrated into MoM, leading to the development of the compressive sensing-based method of moments (CS-MoM) [8]. The core concept of CS-MoM is to transform the matrix equation into CS computational models, thereby enhancing computational efficiency.

CS-MoM includes two computational models. One involves significantly reducing the number of equations to be solved by randomly combining incident excitations from different angles, thus improving computational efficiency for solving monostatic electromagnetic scattering problems [9–12]. The other model constructs an underdetermined equation based on CS theory to solve bistatic electromagnetic scattering problems [13–16]. This method transforms the full-rank matrix equation into a lower-dimensional underdetermined system, thereby significantly reducing both the filling and solution complexities of the matrix equation. This process involves three main steps: constructing the sparse basis, constructing the measurement matrix, and reconstructing the current coefficients. Specifically, the underdetermined equation that satisfies the CS framework is obtained by performing a sparse transformation of the induced current on an appropriate sparse basis and constructing a suitable measurement matrix. Finally, the current coefficients are reconstructed using reconstruction algorithms.

When constructing the sparse basis, Krylov subspace basis functions [15, 17], characteristic basis functions [6, 18], and characteristic mode basis functions (CMBFs) [16, 19] can be used as the sparse basis for analyzing three-dimensional (3D) targets. The construction of CMBFs is independent of the excitation and benefits from domain decomposition methods, making them more suitable for analyzing large-scale electrical problems. Another core technology, constructing the measurement matrix, involves left-multiplying with Gaussian random matrices [13] or randomly extracting [19] certain rows of the impedance matrix. This randomness leads to uncertainty in the computational results. To address this issue, [16] employed uniform extraction to eliminate uncertainties, thereby obtaining stable results. In addition, by constructing an overdetermined system, this method optimizes the reconstruction algorithm from generalized orthogonal matching pursuit (gOMP) [19, 20] to the least squares method, thereby avoiding iterative solving and significantly improving computational efficiency. This led to the development of the novel CS-MoM model (NCS-MoM). However, considering the use of Rao-Wilton-Glisson (RWG) [21] basis functions as testing functions, each testing function corresponds one-to-one with the rows of the impedance matrix. Uniform extraction, however, fails to identify the testing functions that significantly contribute to accuracy. It remains a simple sampling strategy that does not guarantee the acquisition of an optimal measurement

* Corresponding author: Yang Liu (2023200714@aust.edu.cn).

matrix. Therefore, a method capable of identifying these testing functions and providing reliable accuracy is essential.

Unlike previous studies, this paper proposes a dynamic extraction strategy. In particular, the rows of the impedance matrix are ranked in descending order according to the importance of their row norms and then dynamically extracted. The extraction density is higher where the row importance is greater, and lower where the row importance is smaller, ensuring that the matrix is representative, and the global structure is covered.

2. THEORY

The theoretical section primarily consists of three key aspects. First, the CS-MoM computational model is introduced, outlining its three core computational steps: measurement, sparsity, and recovery. Second, the theoretical innovations introduced in the sparsity and recovery stages of the novel CS-MoM model [16] are examined. Finally, the focus shifts to exploring the application advantages and theoretical foundation of the novel measurement matrix proposed in this paper, which serves to enhance the CS-MoM model.

2.1. CS-MoM Framework

The MoM based on RWG basis functions solves the surface integral equation of a 3D target by transforming it into the following matrix equation:

$$\mathbf{ZI} = \mathbf{V} \tag{1}$$

where $\mathbf{Z}$ denotes a full-rank impedance matrix of dimension $N \times N$, and N represents the number of RWG basis functions, that is, the number of unknowns. In addition, $\mathbf{I}$ represents the induced current to be solved, and $\mathbf{V}$ represents the incident excitation of dimension $N \times 1$.

According to CS theory, the measurement matrix $\tilde{\mathbf{Z}}$ is constructed by randomly or uniformly extracting M row elements from the $\mathbf{Z}$ matrix, while the corresponding M rows elements from the $\mathbf{V}$ matrix are extracted as the measurement results $\tilde{\mathbf{V}}$, thereby satisfying the dimensionality reduction requirements of the CS-MoM framework. At this point, the matrix equation in Equation (1) is transformed into an underdetermined equation:

$$\tilde{\mathbf{Z}}\mathrm{I} = \tilde{\mathbf{V}} \tag{2}$$

Considering that the induced current $\mathbf{I}$, discretized using RWG basis functions, is typically not sparse, a sparse transformation is therefore required, as follows:

$$\mathbf{I} = \boldsymbol{\Psi}\boldsymbol{\alpha} \tag{3}$$

where $\boldsymbol{\alpha}$ is the weight coefficient vector, and $\boldsymbol{\Psi}$ is the sparse basis. Therefore, substituting Equation (3) into Equation (2) gives:

$$\tilde{Z}I = \tilde{\mathbf{Z}}\boldsymbol{\Psi}\boldsymbol{\alpha} = \boldsymbol{\Theta}\boldsymbol{\alpha} = \tilde{\mathbf{V}} \tag{4}$$

where $\boldsymbol{\Theta}$ is defined as the sensing matrix of size $M \times N$. At this point, to ensure that $\boldsymbol{\alpha}$ can be solved with high probability, the sensing matrix $\boldsymbol{\Theta}$ needs to satisfy the restricted isometry property (RIP) [22] constraint. In this case, it is sufficient to solve the optimization problem under the l_1-norm:

$$\boldsymbol{\alpha} = \arg\min \|\boldsymbol{\alpha}\|_{l_1} \quad s.t\ \ \boldsymbol{\Theta}\boldsymbol{\alpha} = \tilde{\mathbf{V}} \tag{5}$$

among them, the greedy algorithm is often used to solve Equation (4), and the classical methods include orthogonal matching pursuit algorithm [23] and gOMP algorithm [20].

2.2. Sparse Basis and Recovery Algorithm

According to the characteristic mode (CM) theory of perfect electric conductors (PECs), the 3D target is divided into m blocks. These blocks are then expanded to ensure current continuity, allowing for the solution of the generalized eigenvalue equation constructed [24] from the self-impedance matrix $\mathbf{Z}_{ii}^{e}$ $(i = 1, 2, \cdots, m)$ of each block, thereby obtaining the mode currents:

$$\mathbf{X}_{ii}^{e}\mathbf{J}_{i}^{e} = \lambda_i \mathbf{R}_{ii}^{e}\mathbf{J}_{i}^{e} \tag{6}$$

where $\mathbf{Z}_{ii}^{e} = \mathbf{R}_{ii}^{e} + j\mathbf{X}_{ii}^{e}$. $\mathbf{R}_{ii}^{e}$ and $\mathbf{X}_{ii}^{e}$ represent the matrices consisting of the real and imaginary parts of the extended self-impedance $\mathbf{Z}_{ii}^{e}$ for the ith block, respectively. Furthermore, λ_i and $\mathbf{J}_{i}^{e}$ represent the eigenvalue and their corresponding CM. e indicates extension. Next, after removing the extended region values, the mode currents are truncated based on the mode significance (MS):

$$\mathrm{MS} = \left|\frac{1}{1 + j\lambda_i}\right| \tag{7}$$

Set a truncation threshold τ, and consider the modes corresponding to eigenvalues satisfying $\mathrm{MS} > \tau$ as the valid modes. Let the number of valid modes generated on the ith block be k_i, and these valid modes are then combined as:

$$\mathbf{J}_{i}^{c} = \left[\ \mathbf{J}_{i}^{c} \quad \mathbf{J}_{i}^{c} \quad \cdots \quad \mathbf{J}_{i}^{c}\ \right] \tag{8}$$

After solving for the valid modes on all blocks, the sparse basis $\mathbf{J}^{CM}$ is constructed as follows:

$$\mathbf{I} = \begin{bmatrix} \mathbf{J}_{1}^{c} & \mathbf{0} & \cdots & \mathbf{0} \\ \mathbf{0} & \mathbf{J}_{2}^{c} & \cdots & \mathbf{0} \\ \vdots & \vdots & \ddots & \vdots \\ \mathbf{0} & \mathbf{0} & \cdots & \mathbf{J}_{m}^{c} \end{bmatrix} \boldsymbol{\alpha} = \mathbf{J}^{CM}\boldsymbol{\alpha} \tag{9}$$

where $\mathbf{J}^{CM}$ has dimensions of $N \times K$, with K representing the total number of valid modes across all blocks. Substituting Equation (9) into Equation (4) yields:

$$\tilde{\mathbf{Z}}\mathrm{I} = \tilde{\mathbf{Z}}\mathrm{J}^{CM}\boldsymbol{\alpha} = \boldsymbol{\Theta}\boldsymbol{\alpha} = \tilde{\mathbf{V}} \tag{10}$$

It is worth noting that since the number of columns in the constructed sparse basis is much smaller than the number of unknowns N, Equation (10) forms a smaller overdetermined system. At this point, the least squares method can be used to replace the traditional greedy algorithm for a fast solution of the system, avoiding iteration issues and thereby enabling the reconstruction of the current coefficients:

$$\boldsymbol{\alpha} = \left(\boldsymbol{\Theta}^{T}\tilde{\mathbf{V}}\right) / \left(\boldsymbol{\Theta}^{T}\boldsymbol{\Theta}\right) \tag{11}$$

where $\boldsymbol{\Theta}^{T}$ is the transpose matrix of $\boldsymbol{\Theta}$.

2.3. Measurement Matrix

In the MoM, the impedance matrix $\mathbf{Z}$ is constructed by combining the RWG basis functions with the Galerkin method:

$$\mathbf{Z}=\begin{bmatrix} \langle w_1, L(f_1)\rangle & \langle w_1, L(f_2)\rangle & \cdots & \langle w_1, L(f_N)\rangle \\ \langle w_2, L(f_1)\rangle & \langle w_2, L(f_2)\rangle & \cdots & \langle w_2, L(f_N)\rangle \\ \vdots & \vdots & \ddots & \vdots \\ \langle w_N, L(f_1)\rangle & \langle w_N, L(f_2)\rangle & \cdots & \langle w_N, L(f_N)\rangle \end{bmatrix} \tag{12}$$

$$\mathbf{V}=\begin{bmatrix} \langle w_1, g\rangle \\ \langle w_2, g\rangle \\ \vdots \\ \langle w_N, g\rangle \end{bmatrix} \tag{13}$$

where $(w_m = f_m)$ denotes the test function. $L(\cdot)$ and g represent linear operator and known excitation source, respectively. It can be seen that the CS-MoM model can be considered as a MoM with partial RWG basis function characteristics. Since different testing functions correspond to different spatial and current distributions, they contribute differently to the computational accuracy. As a result, the measurement matrix composed of different rows will lead to different computational outcomes.

It is evident that the random extraction strategy [19] is inadequate for effectively capturing the rows of the impedance matrix $\mathbf{Z}$ that are critical for testing, particularly at low extraction rates. This approach tends to result in unstable computational outcomes due to the lack of a structured way to prioritize the importance of individual rows in the matrix. While random extraction provides diversity in the selected rows, it does not guarantee that the rows with the most relevant information are included in the measurement matrix, which can negatively affect the accuracy and stability of the computation.

In contrast, the sequential extraction method with a fixed step size [16] establishes a unique, deterministic measurement matrix, which can help mitigate the instability inherent in random extraction. The deterministic nature of this method ensures that the rows are extracted in a predictable order, potentially reducing variability. However, this method still faces significant challenges in adequately capturing rows of greater significance. Since it lacks a mechanism to prioritize more informative rows based on their contribution to the impedance matrix, the resulting measurement matrix might fail to include the most critical rows, limiting its effectiveness in capturing the full range of relevant data for precise testing.

To address the limitations of both random and sequential extraction strategies, this paper presents a novel method that constructs the measurement matrix based on the importance of the row norms. By considering the row norms as a measure of their significance, the proposed method selectively extracts the rows that contribute more meaningfully to the impedance matrix. This targeted extraction process ensures that the measurement matrix is not only unique and deterministic but also optimized in terms of the representation of important data. Unlike random extraction, this method prioritizes rows that are more likely to enhance the overall computational accuracy, thus leading to more stable and reliable results. Furthermore, it improves sequential extraction by incorporating a dynamic strategy that adapts to the varying importance of rows, overcoming the challenge of capturing rows with greater significance.

The row norm is an effective indicator for measuring the information contribution of each row in a matrix. In electromagnetic field simulations, different test functions correspond to different spatial and current distributions, with uneven energy distributions. In the impedance matrix, some rows may contain more information or energy, and the computation of these rows has a greater impact on the final solution. By calculating the norm of each row, the influence of these rows on the computational result can be quantified, thereby suggesting that rows with higher information content can be selected and utilized in constructing the measurement matrix. Specifically, the larger the row norm is, the more important the information or energy is carried by that row in the overall computation. Extracting these rows helps improve the accuracy and stability of the model.

For a dense, full-rank impedance matrix $\mathbf{Z}$, the row norm can directly measure the overall energy of each row. The norm of each row can be defined as:

$$E_i = ||\mathbf{Z}_i||_2 = \sqrt{\sum_{j=1}^{N} |\mathbf{Z}_{ij}|^2} \quad \forall i = \{1, \cdots, N\} \tag{14}$$

where $||\mathbf{Z}_i||_2$ represents the 2-norm of the ith row. At this point, the index permutation mapping $\sigma : \{1, \cdots, N\} \rightarrow \{1, \cdots, N\}$ is constructed to satisfy:

$$E_{\sigma(1)} \geq E_{\sigma(1)} \geq \cdots \geq E_{\sigma(N)} \tag{15}$$

Therefore, the ordered index sequence $S = (\sigma(1), \sigma(1), \cdots, \sigma(N))$ is generated, which arranges the energy distribution in a monotonically decreasing order.

Next, the impedance matrix $\mathbf{Z}$ rows are arranged in descending order based on the importance of their row norms, and dynamic extraction is applied. The core idea of dynamic extraction is to arrange the rows of the matrix in descending order based on the importance of their row norms, followed by applying a decreasing extraction density. Specifically, dense extraction is performed for rows with higher $||\mathbf{Z}_i||_2$, while sparse extraction is applied to rows with lower $||\mathbf{Z}_i||_2$. This strategy ensures the matrix's representativeness while avoiding information loss. The following is the formula for dynamic extraction:

$$\Delta(K) = S_0 + K(S_f - S_0)/N \tag{16}$$

where $\Delta(K)$ represents the dynamic extraction steps, rounded up, while S_0 and S_f denote the starting and ending extraction steps, respectively. In addition, the schematic of the dynamic extraction of the impedance matrix based on row norm importance is shown in Figure 1. It can be seen that the extraction process follows a transition from dense to sparse according to the importance of row norms.

Finally, to clearly demonstrate the extraction process of the proposed method, Figure 2 illustrates both the extraction strategy and its correction completeness. Specifically, Figure 2(a)

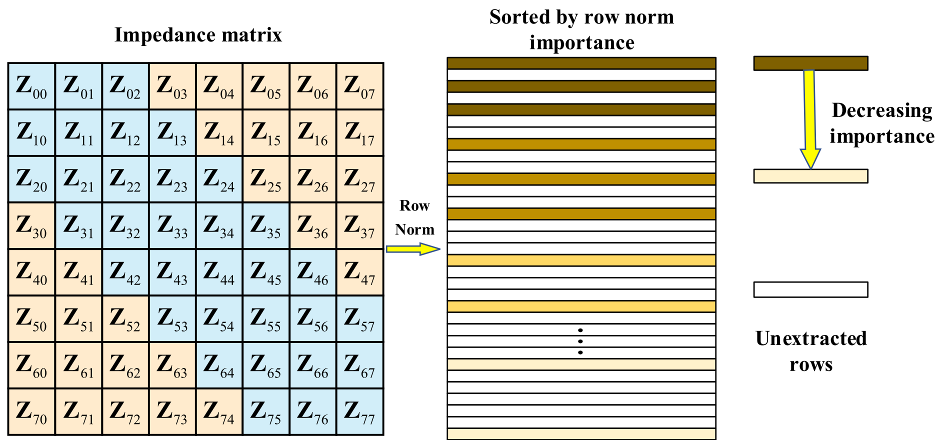

FIGURE 1. Schematic of dynamic extraction of the impedance matrix based on row norm importance.

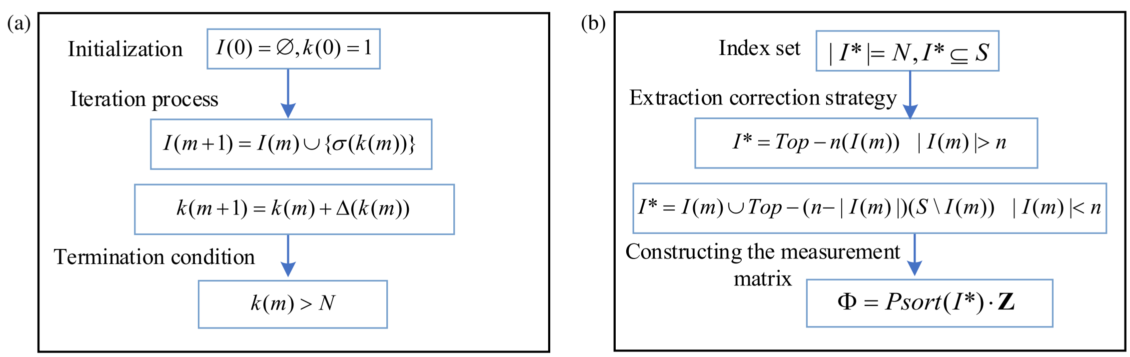

FIGURE 2. The algorithm flow for constructing the measurement matrix of the proposed method. (a) Iterative mapping of row index selection for the measurement matrix. (b) The extraction correction strategy of the proposed method.

depicts the iterative mapping process used to extract the row indices for the measurement matrix, while Figure 2(b) shows the correction process implemented to ensure the completeness of the extraction during the construction of the measurement matrix.

3. NUMERICAL RESULTS

Different objects are simulated and analyzed to test the proposed method's effectiveness. The accuracy was evaluated using the root mean square error (RMSE) of the radar cross section (RCS), which is defined as follows:

$$\mathrm{RMSE}=\sqrt{\frac{1}{N_a}\sum_{i=1}^{N_a}\left|\mathrm{RCS}_{cal,i}-\mathrm{RCS}_{ref,i}\right|^2} \tag{17}$$

where $\mathrm{RCS}_{cal,i}$ is the calculation result of the method used, $\mathrm{RCS}_{ref,i}$ the calculation result using MoM, and N_a the number of sampling points.

3.1. Perfect Electrical Conductor Missile

Firstly, the bistatic RCS was investigated for a PEC missile model with a side length of 1 m; the frequency of the incident plane wave is set to 2 GHz; and the observed scattering angle is $(\theta,\varphi)=(0°\text{–}360°, 0°)$, where θ and φ represent the zenith and azimuth angles, respectively. By utilizing RWG basis functions, the cube's surface is discretized into 12728 triangles, leading to 19092 unknowns. Additionally, the target is divided into 8 blocks, with each extended by 0.15 wavelength, resulting in 24569 unknowns. The threshold τ for the MS method is set to 0.001, yielding 1811 CMs.

First, Table 1 presents the correlation coefficients between the measurement matrix $\tilde{\mathbf{Z}}$ and sparse matrix $\mathbf{J}^{CM}$ constructed using the random extraction and uniform extraction strategies, as well as the proposed method. It is evident that the measure-

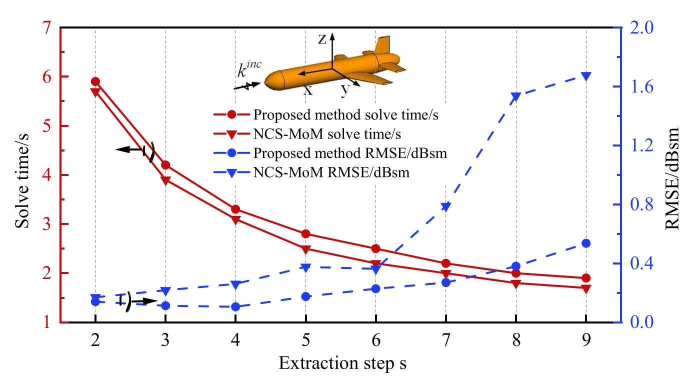

FIGURE 3. The time and RMSE for different extraction steps of the missile model.

TABLE 1. Correlation coefficients between measurement matrix and sparse basis.

Method	Random extraction	Uniform extraction	Proposed method
Correlation coefficient	$0.0041 + 0.1677i$	$0.1117 - 0.0131i$	$0.0050 + 0.1237i$

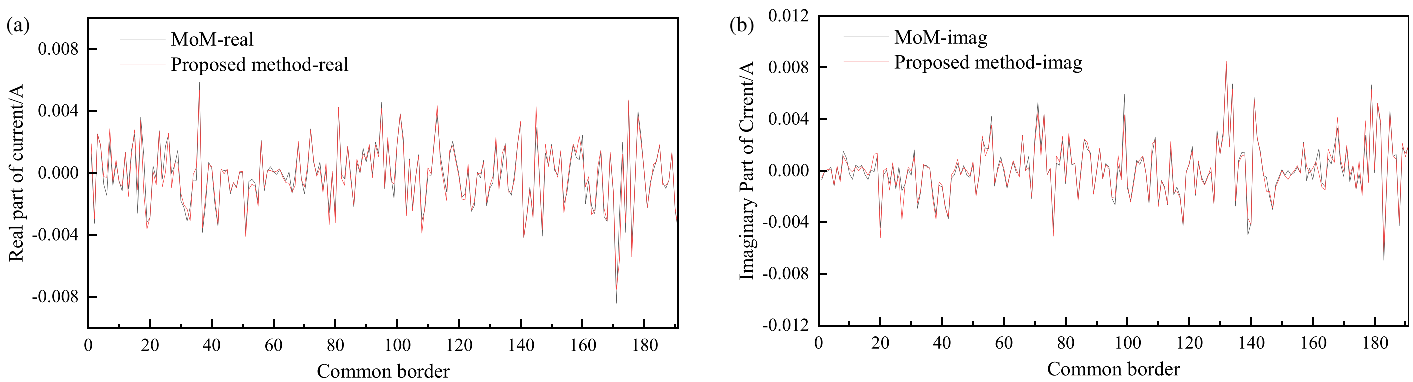

FIGURE 4. Common border currents. (a) Current real part. (b) Current imaginary part.

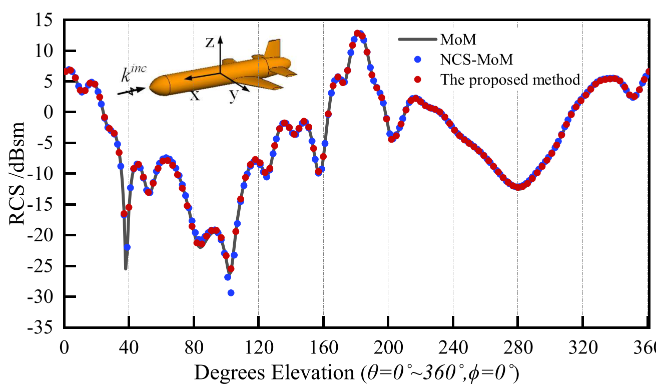

FIGURE 5. Bistatic RCS of the missile in horizontal polarization.

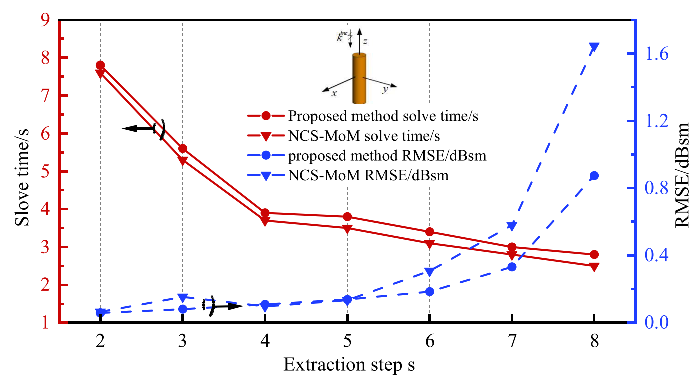

FIGURE 6. The time and RMSE for different extraction steps of the cylinder model.

ment matrix $\tilde{\mathbf{Z}}$ constructed using the proposed method exhibits a weak correlation with the sparse transformation matrix $\mathbf{J}^{CM}$, satisfying the RIP [23], which ensures the accurate reconstruction of the sparse coefficient $\boldsymbol{\alpha}$.

To validate the advantage of the proposed method over NCS-MoM in terms of computational accuracy, Figure 3 illustrates the solution time and RMSE corresponding to two different extraction methods at various extraction steps. The number of rows for the dynamic extraction step in the proposed method is consistent with that of uniform extraction. The solution time includes the matrix equation construction and current recovery. As shown in Figure 3, the computational times for both methods are similar. Still, the RMSE of the proposed method is consistently lower than that of uniform extraction, indicating higher computational accuracy. This advantage becomes particularly pronounced when the extraction step exceeds 6.

To further validate the accuracy of the proposed method, Figure 4 compares the current results obtained from both the proposed method and MoM calculations. The currents shown in the figure are extracted uniformly, with 19092 common edge currents and a step size of 100. As illustrated in Figures 4(a) and 4(b), representing the real and imaginary parts, respectively, the currents recovered using the proposed method closely match those obtained from MoM calculations. Additionally, Figure 5 presents the RCS results for both the NCS-MoM and proposed method, with uniform extraction steps of 5. The proposed method produces horizontally polarized RCS results for the missile that closely align with the MoM results.

3.2. Perfect Electrical Conductor Cylinder

Secondly, to further demonstrate the benefits of the proposed method. The bistatic RCS of a PEC cylinder model with a base radius of 0.5 m and a height of 1 m is analyzed. The frequency of the incident wave is set to 900 MHz, and the observed scattering angle is $(\theta, \varphi) = (0°–360°, 0°)$. The target surface is discretized into 14658 triangles, which produces 21987 unknowns, and the target is divided into 8 blocks, generating 2316 CMs. Moreover, each block is expanded in all directions according to 0.15 wavelength, and the number of unknowns after extension is 31924.

As seen in Figure 6, the proposed method still outperforms uniform extraction in terms of computational accuracy for the

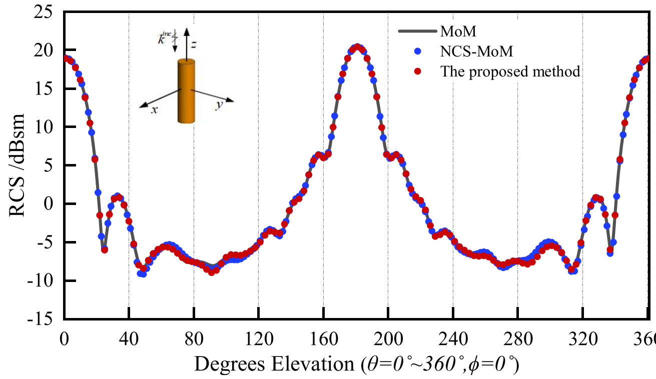

FIGURE 7. Bistatic RCS of the cylinder in horizontal polarization.

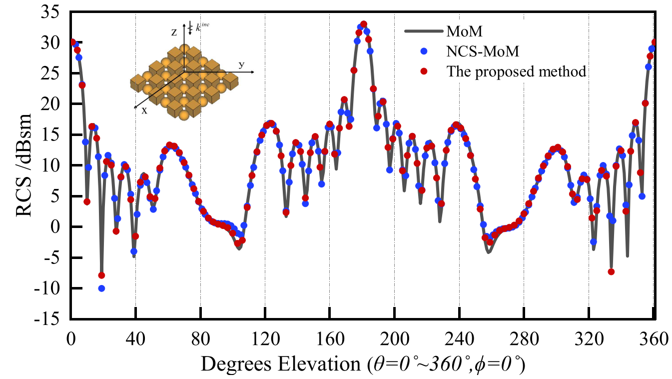

FIGURE 8. Bistatic RCS of the array target in horizontal polarization.

TABLE 2. Simulation time and accuracy.

Model	Method	Unknown	Construction time of sparse basis (s)	Recovery induced current time (s)	Total time (s)	RMSE (dBsm)
Missile	NCS-MoM	19092	51.19	2.57	53.76	0.38
	Proposed method		51.19	2.86	54.05	0.17
Cylinder	NCS-MoM	21987	78.80	3.16	81.96	0.31
	Proposed method		78.80	3.42	82.22	0.18
Array target	NCS-MoM	77976	578.32	91.69	670.01	0.53
	Proposed method		578.32	93.51	671.83	0.32

cylinder model. Consistent with the missile model, the advantage becomes more pronounced when the extraction step exceeds 6. Furthermore, the RCS results of the three methods are shown in Figure 7, which shows that the proposed method matches well with the MoM, and the calculation accuracy is high.

3.3. Perfect Electrical Conductor Array Target

Thirdly, the scattering problem of an array target consisting of 36 PEC objects with two different shapes is analyzed to further investigate the proposed method's effectiveness on large targets. The frequency of the incident plane wave is set to 800 MHz, and the observed scattering angle is $(\theta, \varphi) = (0°–360°, 0°)$. Meanwhile, the surface of the array target is discretized into 51984 triangles using RWG functions, resulting in 77976 unknowns. The target is then divided into 36 blocks, generating 6776 CMs. In addition, Figure 8 presents the bistatic RCS results computed using the three methods, with the uniform extraction step set to 5 and the number of rows extracted by the proposed method remaining consistent. As shown in Figure 8, the RCS results obtained using the proposed method closely align with the MoM results.

Finally, Table 2 demonstrates a comparative analysis of computation time and RCS error between NCS-MoM and the proposed method across three different models. It is worth noting that the recovery time of the current includes both matrix equation construction and current reconstruction steps. Analyzing the table results reveals that the proposed method achieves improved computational accuracy for all three target types at only a marginal time cost, achieving respective improvements of 55.3%, 41.9%, and 39.6% in solution precision.

4. CONCLUSION

This paper presents a novel measurement strategy to enhance the performance of CS-MoM. By introducing row norm importance, the rows of the impedance matrix are ranked in descending order. Dynamic extraction is then employed to perform dense and sparse extraction, which improves computational accuracy compared to uniform extraction. Experimental simulations are conducted to validate the theoretical feasibility of the proposed method.

ACKNOWLEDGEMENT

This work was supported in part the Natural Science Research Project of Anhui Educational Committee under No. 2022AH051583, in part by the Graduate Innovation Fund of Anhui University of Science and Technology under grant No. 2024cx2062.

REFERENCES

[1] Harrington, R. F., *Field Computation by Moment Methods*, Macmillan, New York, 1968.

[2] Song, J., C.-C. Lu, and W. C. Chew, "Multilevel fast multipole algorithm for electromagnetic scattering by large complex objects," *IEEE Transactions on Antennas and Propagation*, Vol. 45, No. 10, 1488–1493, Oct. 1997.

[3] Jorgensen, E., J. L. Volakis, P. Meincke, and O. Breinbjerg, "Higher order hierarchical legendre basis functions for electromagnetic modeling," *IEEE Transactions on Antennas and Propagation*, Vol. 52, No. 11, 2985–2995, Nov. 2004.

[4] Prakash, V. V. S. and R. Mittra, "Characteristic basis function method: A new technique for efficient solution of method of moments matrix equations," *Microwave and Optical Technology Letters*, Vol. 36, No. 2, 95–100, Jan. 2003.

[5] Lucente, E., A. Monorchio, and R. Mittra, "An iteration-free MoM approach based on excitation independent characteristic basis functions for solving large multiscale electromagnetic scattering problems," *IEEE Transactions on Antennas and Propagation*, Vol. 56, No. 4, 999–1007, Apr. 2008.

[6] Wang, P., Z.-G. Wang, Y.-F. Sun, and W.-Y. Nie, "Novel compressive sensing computing model used for analyzing electromagnetic scattering characteristics of three-dimensional electrically large objects," *Acta Physica Sinica*, Vol. 72, No. 3, 54–61, Feb. 2023.

[7] Donoho, D. L., "Compressed sensing," *IEEE Transactions on Information Theory*, Vol. 52, No. 4, 1289–1306, Apr. 2006.

[8] Chen, M. S., F. L. Liu, H. M. Du, and X. L. Wu, "Compressive sensing for fast analysis of wide-angle monostatic scattering problems," *IEEE Antennas and Wireless Propagation Letters*, Vol. 10, 1243–1246, Oct. 2011.

[9] Chai, S.-R. and L.-X. Guo, "A new method based on compressive sensing for monostatic scattering analysis," *Microwave and Optical Technology Letters*, Vol. 57, No. 10, 2457–2461, Oct. 2015.

[10] Chai, S.-R. and L.-X. Guo, "Compressive sensing for monostatic scattering from 3-D NURBS geometries," *IEEE Transactions on Antennas and Propagation*, Vol. 64, No. 8, 3545–3553, 2016.

[11] Kong, M., M. Chen, X. Cao, L. Zhang, Q. Qi, and X. Wu, "Fast analysis of local current distribution for electromagnetic scattering problems of electrically large objects," *IEEE Access*, Vol. 8, 127 640–127 647, Jul. 2020.

[12] Kong, M., M. S. Chen, X. Y. Cao, J. B. Zhu, X. J. Kuang, Q. Qi, and X. L. Wu, "Fast electromagnetic scattering analysis of inhomogeneous dielectric objects over a wide incident angle," *IEEE Antennas and Wireless Propagation Letters*, Vol. 20, No. 8, 1527–1531, Aug. 2021.

[13] Chai, S.-R. and L.-X. Guo, "Fast analysis of bistatic scattering problems with compressive sensing technique," *Journal of Electromagnetic Waves and Applications*, Vol. 30, No. 13, 1755–1762, 2016.

[14] Kong, M., M. S. Chen, B. Wu, and X. L. Wu, "Fast and stabilized algorithm for analyzing electromagnetic scattering problems of bodies of revolution by compressive sensing," *IEEE Antennas and Wireless Propagation Letters*, Vol. 16, 198–201, May 2016.

[15] Wang, Z., H. Yuan, Y. Sun, W. Nie, and P. Wang, "Block-based Krylov subspace basis functions for solving bistatic scattering problems," *IEEE Antennas and Wireless Propagation Letters*, Vol. 22, No. 10, 2561–2565, Oct. 2023.

[16] Gao, Y., M. F. Akbar, and G. N. Jawad, "Stabilized and fast method for compressive-sensing-based method of moments," *IEEE Antennas and Wireless Propagation Letters*, Vol. 22, No. 12, 2915–2919, Dec. 2023.

[17] Cao, X., M. Chen, Q. Qi, M. Kong, J. Hu, L. Zhang, and X. Wu, "Solving electromagnetic scattering problems by underdetermined equations and Krylov subspace," *IEEE Microwave and Wireless Components Letters*, Vol. 30, No. 6, 541–544, Jun. 2020.

[18] Wang, Z.-G., W.-Y. Nie, and H. Lin, "Characteristic basis functions enhanced compressive sensing for solving the bistatic scattering problems of three-dimensional targets," *Microwave and Optical Technology Letters*, Vol. 62, No. 10, 3132–3138, May 2020.

[19] Wang, Z., P. Wang, Y. Sun, and W. Nie, "Fast analysis of bistatic scattering problems for three-dimensional objects using compressive sensing and characteristic modes," *IEEE Antennas and Wireless Propagation Letters*, Vol. 21, No. 9, 1817–1821, Sep. 2022.

[20] Wang, J., S. Kwon, and B. Shim, "Generalized orthogonal matching pursuit," *IEEE Transactions on Signal Processing*, Vol. 60, No. 12, 6202–6216, Sep. 2012.

[21] Rao, S., D. Wilton, and A. Glisson, "Electromagnetic scattering by surfaces of arbitrary shape," *IEEE Transactions on Antennas and Propagation*, Vol. 30, No. 3, 409–418, 1982.

[22] Candès, E. J., "The restricted isometry property and its implications for compressed sensing," *Comptes Rendus Mathématique*, Vol. 346, No. 9-10, 589–592, 2008.

[23] Tropp, J. A. and A. C. Gilbert, "Signal recovery from random measurements via orthogonal matching pursuit," *IEEE Transactions on Information Theory*, Vol. 53, No. 12, 4655–4666, 2007.

[24] Harrington, R. and J. Mautz, "Theory of characteristic modes for conducting bodies," *IEEE Transactions on Antennas and Propagation*, Vol. 19, No. 5, 622–628, 1971.